Journal of Computational Acoustics, Vol. 25, No. 4 (2017) 1750029 (16 pages)
© IMACS
DOI: 10.1142/S0218396X17500291

INTERNATIONAL ASSOCIATION
FOR MATHEMATICS AND
COMPUTERS IN SIMULATION

Diffusion Equation-Based Finite Element Modeling of a Monumental Worship Space

Zühre Sü Gül*, Ning Xiang† and Mehmet Çalışkan‡
*MEZZO Stüdyo Ltd, Turkey
†Graduate Program in Architectural Acoustics
School of Architecture, Rensselaer Polytechnic Institute, USA
‡Department of Mechanical Engineering
Middle East Technical University, Turkey
*zuhre@mezzostudyo.com

Received 1 June 2016
Accepted 17 March 2017
Published 25 April 2017

In this work, a diffusion equation model (DEM) is applied to a room acoustics case for in-depth sound field analysis. Background of the theory, the governing and boundary equations specifically applicable to this study are presented. A three-dimensional geometric model of a monumental worship space is composed. The DEM is solved over this model in a finite element framework to obtain sound energy densities. The sound field within the monument is numerically assessed; spatial sound energy distributions and flow vector analysis are conducted through the time-dependent DEM solutions.

Keywords: Diffusion equation model; finite element method; room acoustics.

1. Introduction

The aim of this study is to investigate the sound field of a monumental worship structure by applying a diffusion equation model (DEM) in room acoustics predictions. The DEM is implemented within a finite-element framework for detailed analysis of sound energy flows between different subvolumes of the structure. Many different methods have previously been developed for sound field investigations in room acoustics, which is a branch of acoustics that deals with acoustical fields inside enclosed environments. Among these enclosures, conference halls, multi-purpose auditoria, concert halls, opera houses and worship spaces most commonly necessitate detailed acoustical design. Especially in design phase of such speech or music-related venues, or for in-depth experimental analysis, theoretical models are utilized.

Classical theories applied in room acoustics estimations and simulations include statistical acoustics,[1,2] wave theory,[3–6] geometrical room acoustics,[6,7] statistical energy analysis,[8]

acoustic radiosity,[9–11] and most recently, diffusion equation model application.[12–16] Different models have different limitations, Savioja and Svensson have published the most recent overview on this research field,[6] yet excluding the diffusion theory[12–16] and the transport theory for room acoustic simulations.[17–20]

The main difference between classical statistical acoustics and the diffusion equation model is that the DEM allows for modeling the spatial variation of the reverberant sound field, while the statistical model estimates yield only one single value for each room under the diffusion sound field assumption. Therefore, the DEM represents a higher order of the statistical acoustics in room acoustics.[16] The diffusion model, which takes the sound source location, room geometry and different surface properties into account, is able to predict spatial variations/distributions of sound energy, while the statistical acoustics theory does not. On the other hand, the DEM assumes sound particles travel along straight lines at the speed of sound. A recent work using the energy radiative transport equation[17,18] describes the theoretical framework of a geometrical sound particle approach which can asymptotically be reduced to the diffusion equation model,[19,20] so the DEM is also governed by geometrical acoustics theory. The major advantage of the DEM over conventional geometrical acoustics approaches is its computational efficiency in numerical implementations. One reason for that is ray-tracing-based algorithms spend entire computational effort to provide a solution only for one single source-receiver configuration, for multiple positions, while the DEM inherently provide all the solutions on every finite-element grid points within one complete computation run. The DEM can be solved using different mediums. In this paper, finite element method is utilized. Another approach is applying finite difference method.[21,22]

Local reverberant sound energy densities in rooms with diffuse reflecting boundaries can be described as diffusion processes in analogy to heat transport in solids originated by Fourier,[23] or light energy propagating through scattering media,[24] both of which are based on the mathematical theory of diffusion. This model has also been found suitable to predict reverberant sound energy in arbitrarily shaped enclosures with nonhomogeneous distribution of boundary absorption.[25]

The numerical implementation of the DEM in room acoustics predictions is thoroughly studied by Valeau *et al.*[13] Their results point out the possibility of this new model to be a solution of various room shapes. Billon *et al.*[14] applied the diffusion model for the coupled volume configuration, their results are compared with experimental data, with statistical theory and a ray-based model. Mean sound pressure level of the reverberant field is obtained from the diffusion model. The obtained solution allows the estimation of the sound decay and consequently the decay times at any location in the rooms. Jing and Xiang[26] have taken a step forward to extend the DEM for high absorption cases so that some surfaces of the room under test could be sound absorptive. Authors used an Eyring absorption term for the boundary condition, whereas previous models are only for rooms with low absorptive interior surfaces. Billon *et al.*[27] have also independently applied the Eyring absorption model for solving the DEM in nonuniformly absorbing rooms. They have supported the argument

using Eyring model by experiments on real cases, specifically a reverberation chamber with sound absorptive patches of glass wool.

Jing and Xiang[28] applied the DEM to coupled-volume systems to visualize sound flow directions (vectors). A finite element solver is used for numerical implementation. A singularity problem with the Eyring coefficient in the DEM boundary term, in rooms with local surfaces having an absorption coefficient of unity, is eliminated by the modified boundary condition developed by Jing and Xiang.[15] Simulations and scale model tests were conducted for comparisons and reliability analysis of the new boundary term. Xiang *et al.*[29] carried out another study on the DEM revealing sound energy distributions and energy feedback across the coupling aperture in the coupled volume systems. These authors[15,29] proposed a new absorption term in boundary conditions associated with the DEM which can handle high absorption for some small portions of interior surfaces. Their experimental scale model results reveal sound energy feedback in coupled-volume systems in terms of modeling sound energy flow vectors.

A shortcoming of the DEM is that the model is only valid in later time segments of an impulse response (late reverberation). According to Xiang *et al.*[22] and Escolano *et al.*[30] studies, direct sound and early reflections in initial time steps do not create diffuse field conditions, therefore, the DEM does not yield prediction results for this early part. The very first time intervals should be taken out of the impulse response data so as to ensure reliable DEM analysis. Their study reveals that the DEM is valid after two or more mean free times, the time associated with the mean free path length. Xiang *et al.*[22] recently carried out a systematic study using the DEM in sound fields of coupled volume systems. It reveals that the DEM is only valid to predict reverberation in the later time instance (after the diffuse sound field is established, or at least two or three mean free times (MFTs)); even when the overall surface absorption is as high as 0.48, yet the accurate modeling of the reverberation process becomes valid at even later time instants, 6–8 MFTs later.

In this study, a real-size monumental worship space, for the first time, is investigated using the diffusion equation model for in-depth sound field analysis. This paper is structured as follows, Sec. 2 describes the fundamental theory of the diffusion equation model that heavily relies on recent work by Valeau[13] and Jing and Xiang.[15] In this section, interior and boundary equations and technical details of a finite-element solution using the COMSOL® solver are provided. Section 3 discusses modeling results of the historically significant worship space by spatial sound energy distribution and flow vector analysis. Section 4 concludes the paper by emphasizing the major outcomes of this study.

2. Theory of the Diffusion Equation Model

This section presents the governing and boundary equations within scope of the DEM that fits most properly to enclosures with proportionate dimensions. The room acoustics DEM is based on the sound particle concept under the assumption[12,20,25,31] that particles travel along straight lines at the speed of sound in the interior space and multiple diffuse reflections occur on the room boundaries which can be conceived as scattering objects. These diffuse

reflections of the sound particles will establish a reverberation process building up a so-called diffuse sound field in the enclosure under test, such that the evolution of this diffuse sound field can be described as a diffusion process.

2.1. *Interior diffusion equation*

When interior surfaces of an enclosure are diffusely reflecting, the sound energy flow vector $\mathbf{J}$ caused by the gradient of the sound energy density w at position ($\mathbf{r}$), and time (t) can be expressed by Fick's law[12,31]

$$\mathbf{J}(\mathbf{r},t) = -D \text{ grad } w(\mathbf{r},t) \tag{1}$$

where D is the diffusion coefficient, which takes into account the room morphology via its mean free path (λ)[13] given by

$$D = \frac{\lambda c}{3} = \frac{4Vc}{3S}, \tag{2}$$

where V is the volume of the room and S is the total surface area of the room. Under assumption that the sound energy density w in a region (domain V) excluding sound sources changes per unit time[15] as

$$\frac{\partial w(\mathbf{r},t)}{\partial t} = -\text{div}\mathbf{J}(\mathbf{r},t) = D\nabla^2 w(\mathbf{r},t), \quad \in V, \tag{3}$$

where Eq. (1) is used to arrive at the right-hand side of Eq. (3). ∇^2 is Laplace operator. In the presence of an omni-directional sound source within a room region or domain (V) with time-dependent energy density, Eq. (3) has to take the omni-directional sound source, $q(\mathbf{r},t)$, into account[13]

$$\frac{\partial w(\mathbf{r},t)}{\partial t} = q(\mathbf{r},t) + D\nabla^2 w(\mathbf{r},t), \quad \in V. \tag{4}$$

The sound energy density changing with time may partially be caused by the air dissipation, so as to include the air dissipation as energy losses

$$\frac{\partial w(\mathbf{r},t)}{\partial t} = q(\mathbf{r},t) + D\nabla^2 w(\mathbf{r},t) - cmw(\mathbf{r},t), \quad \in V, \tag{5}$$

where c is speed of sound and m is the coefficient of air absorption.

In Eq. (5), the source term $q(\mathbf{r},t)$ is zero for any subdomain in which no source is present. In a time-dependent solution, a point source with an arbitrary acoustic power of $P(t)$ can be modeled as an impulsive sound source as follows:

$$q(\mathbf{r}_s,t) = E_0\delta(\mathbf{r}-\mathbf{r}_s)\delta(t-t_0), \tag{6}$$

where δ is the Dirac-delta function, $\mathbf{r}_s$ denotes the position of the source. E_0 is the energy produced by the source at source location $\mathbf{r}_s$ and at time t_0. For practical purposes, a source emitting a constant power P in a short time interval Δt can be considered. Thus, E_0 can be approximated by $E_0 \simeq P\Delta t$.[13]

2.2. *Boundary conditions*

The diffusion equation is defined for 'inside the domain (V)' in the previous section. The effects of enclosing room surfaces can analytically be expressed by boundary equations defined for 'on the boundary surfaces (S)'. If the sound energy in an enclosure/domain (V) cannot escape from bounded surfaces (S), then the boundary condition equation[13] becomes

$$\mathbf{J}(\mathbf{r},t)\cdot\mathbf{n} = -D\nabla w(\mathbf{r},t)\cdot\mathbf{n} = 0, \quad \text{on } V, \tag{7}$$

where $\mathbf{n}$ is the surface outgoing normal, D is again the 'diffusion coefficient' and $w(\mathbf{r},t)$ is the acoustic energy density at a position ($\mathbf{r}$) and time (t). The position ($\mathbf{r}$) is specifically on the interior surfaces. Equation (7) is a so-called homogeneous Neumann boundary condition.[13] The boundary condition established to include energy exchanges on enclosing surfaces is

$$\mathbf{J}(\mathbf{r},t)\cdot\mathbf{n} = -D\nabla w(\mathbf{r},t)\cdot\mathbf{n} = A_X c w(\mathbf{r},t), \quad \text{on } S, \tag{8}$$

where A_X is an exchange coefficient or the so-called *absorption factor* which is expressed as follows:

$$A_X = A_S = \frac{\alpha}{4}, \tag{9}$$

where α is the absorption coefficient of the specific surface/boundary. The subscript S of A_S is used to denote Sabine absorption. The diffusion equation model with this boundary condition is accurate only for modeling rooms with low absorption. To improve the accuracy of mixed boundary conditions associated with high absorption for specific room surfaces, the Sabine absorption coefficient in the absorption factor is replaced by the Eyring absorption coefficient as[26,27]

$$A_X = A_E = \frac{-\log(1-\alpha)}{4}. \tag{10}$$

The subscript E of A_E is used to denote Eyring absorption. There exists a singularity within the diffusion-Eyring model given in Eq. (10), when the absorption coefficient for a surface in the frequency of interest becomes 1.0. For resolving the singularity problem with the Eyring model, a modified boundary condition is introduced.[15] This modified absorption factor term can be applied for mixed boundary conditions or more specifically for modeling the local effects of the sound fields that have comparatively higher absorption on specific surfaces, as given by[15]

$$A_X = A_M = \frac{\alpha}{2(2-\alpha)}. \tag{11}$$

In the current case of the worship space, given the fact that the room has a carpet floor that is absorptive in specific octave bands, versus a low absorptive/reflective upper shell, its boundary conditions are best described by the modified mixed boundary model. Thus, combining Eqs. (8) and (11) gives the resulting system boundary equation

$$-D\frac{\partial w(\mathbf{r},t)}{\partial n} = \frac{c\alpha}{2(2-\alpha)} w(\mathbf{r},t), \quad \text{on } S. \tag{12}$$

Equations (5), (6) and (12) are applied to obtain the time-dependent solution. Resulting $w(\mathbf{r}, t)$'s after conversion of sound energy into sound level (SL) in decibels, where $[\log_{10} w]$ is logarithm to the base 10, are used for spatial sound energy density distribution as indicated in Eq. (13).

$$\mathrm{SL} = 10 * \log_{10}(w(\mathbf{r}, t)). \tag{13}$$

Fick's law expressed in Eq. (1) is employed in the following to investigate sound energy flow vector analysis.[32]

3. Numerical Implementation in a Worship Space

In order to validly apply the above described diffusion equation in room acoustic scenarios,[20] the scattering sound particle density must be high, and the reflection of energy must dominate over absorption in the space under investigation. This historically significant venue in the current study falls within this principal assumption, the interior of the venue features rich decorative (diffusion) elements, ornamentation, arches, columns, and the majority of the interior surfaces are also highly reflective. Only a small portion of the interior surfaces is covered by low-absorptive carpet with an absorption coefficient as low as 0.23, yet the overall room absorption coefficient amounts to 0.12, *for* 1 kHz.

The basis of the finite element method is the representation of a body or a structure by an assemblage of subdivisions called finite elements. The finite element method translates partial differential equation problems into a set of linear algebraic equations. The mesh settings determine the resolution of the finite element mesh used to discretize the model in one, two or three dimensions. The advantage of the DEM in room acoustics is that the meshing condition does not depend on the wavelength, rather the mean free path in defining mesh size. As long as the maximum mesh size is smaller than the mean free path of the room, the DEM can be applied with high computational efficiency for a range of frequencies. In application of the DEM analysis over the monumental worship space, a sufficiently detailed interior geometry of the space is imported in a commercial finite element solver software, namely, COMSOL® Multi-physics.

The geometric model of the worship space is divided into 124 788 linear Lagrange-type mesh elements (Fig. 1). The maximum size should be user defined in order not to exceed the mean free path (MFP), while the minimum size depends on the geometrical attributes of the space under consideration. For instance, the transitions between domes and adjacent arches in this model create smaller surfaces requiring smaller mesh sizes at those locations. A pure cubical form could be meshed with larger sized and fewer numbers of elements. As indicated in the previous literature,[12,13,25,29] the meshing condition in DEM is based only on the MFP (1/6 of the MF).[13] Maximum mesh element sizes should be smaller than the MFP. In this study, the minimum mesh element size is 1.12 m and maximum is 6.20 m. So the range is in between 1/3 to 1/16 of MFP. For smaller surfaces as of pendentive connections to main dome, surfaces get smaller than the maximum mesh size and the meshing gets smaller. Using smaller meshes only increases the computational expense of simulation. As

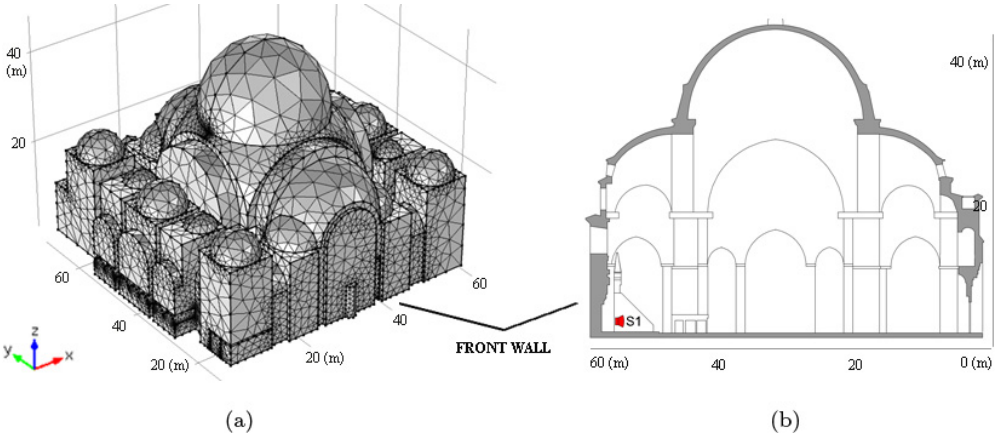

Fig. 1. (a) Solid mesh model of the monument, the entire interior volume is meshed into 124 788 linear Lagrange-type mesh elements with sizes ranging between 1.12 m and 6.2 m. (b) Section view with source (S1) location.

long as the maximum mesh size criteria is satisfied than DEM is applicable for the sake of reducing the computational expenses.

The inner plan of the monument is a rectangle measuring 63 m × 69 m. The height of the dome from the ground to the keystone is 47.75 m, which gives an interior volume $\simeq$ 129 000 m^3. The interior surface area is 28 258 m^2. According to Eq. (2), the MFP of the room is estimated to be 18.26 m and the MFT of the room is 0.053 sec (53 msec). It is known that DEM is valid when statistical and geometrical room acoustics are valid. The overall reverberation time at 250 Hz amounts to 12 sec (Fig. 2), so the Schroeder frequency estimates to 19 Hz. Considering the large scale/size and interior dimensions of the monument, DEM solutions for frequency range above and including 250 Hz are found reliable and thus presented under Sec. 4. Xiang *et al.*[29] also reported that the diffusion equation model can be considered as valid after at least two or three MFP times. In this case, two MFTs correspond to 0.1 sec and three MFTs correspond to 0.15 sec, so all the results of energy

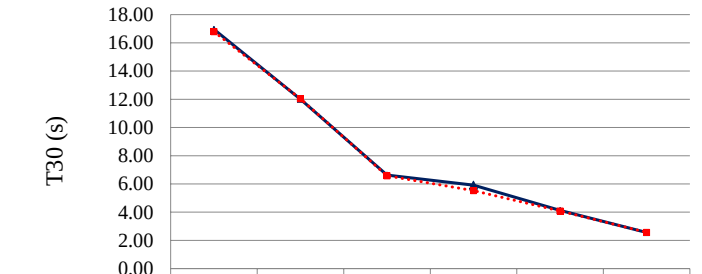

	125Hz	250Hz	500Hz	1kHz	2kHz	4kHz
Field Tests	16.96	12.01	6.63	5.91	4.12	2.56
Simulation	16.79	12.04	6.58	5.53	4.08	2.57

Fig. 2. Reverberation time (T_{30}) comparison of field tests and simulations over 1/1 octave bands.

Table 1. Interior finish materials' sound absorption coefficients over 1/1 octave bands.

Material	125 Hz	250 Hz	500 Hz	1 kHz	2 kHz	4 kHz
Lime-based plastered brick	0.03	0.05	0.15	0.18	0.20	0.23
Marble	0.01	0.01	0.01	0.01	0.02	0.02
Carpet	0.08	0.15	0.17	0.23	0.41	0.59

density distributions or energy flux are considered as to be 0.2 sec after the direct sound arrival.

In DEM simulations, the absorption coefficients of locational surfaces can be assigned to have different absorption coefficients. The upper structure of the case building is finished with lime-based plaster painted brick and marble, while the floor is carpet. In the model, the relevant sound absorption coefficient data for each octave band is assigned to the absorption terms of the boundary equations, specific to local surface materials of interior boundary layers. The absorption coefficients assigned to the materials applied within the monument are given in Table 1.

It should be noted that prior to simulation studies field measurements were taken within the monument.[33] Before implementation of DEM simulation, initially the model is fine-tuned with field test results taking into account the reverberation time (T_{30}) (Fig. 2). Sound source is located in front of front/mihrab wall at the central axis at a height of 1.5 m (Fig. 1(b)). The time-dependent DEM solutions are obtained under the impulsive source excitation, providing the spatial sound energetic room impulse responses to derive the sound density and sound energy flow vector distributions. For such a huge volume, the time-dependent simulation takes approximately 3 h on a computer with Intel(R) Core(TM) i5 CPU, M540@2.53 GHz processor.

4. Sound Energy Distribution and Flow Vector Analysis

Over the geometric model of the monumental worship space, a time-dependent DEM solution is obtained. Throughout the entire interior volume, spatial sound energy distribution levels (in dB), and sound energy flow vector analysis results are available based on Eq. (1).[32] In the following, results are summarized for selected octave bands; for 250 Hz (Figs. 3–7) and for 1000 Hz (Figs. 8–12) over axonometric, plan and section views. To prevent unnecessary repetition of data, specific times are selected for illustrating common trends, as other time intervals are either identical or very close to the prior/following time steps.

Figure 3 illustrates spatial sound energy level distributions out of the DEM solutions in terms of volume and slice plots as well as flow vectors/array plots for 250 Hz at a time of 0.1 sec. This time instant indicates the ignition of the impulsive sound source. The point source is located in front of the *mihrab* wall, where the energy starts flowing from that location towards the upper domical shelter and side walls. At this time instant, the concentration of sound energy density is at the front part of the *mihrab* wall, where the point source is defined. The energy starts to flow from the *mihrab* wall towards the back of the prayer

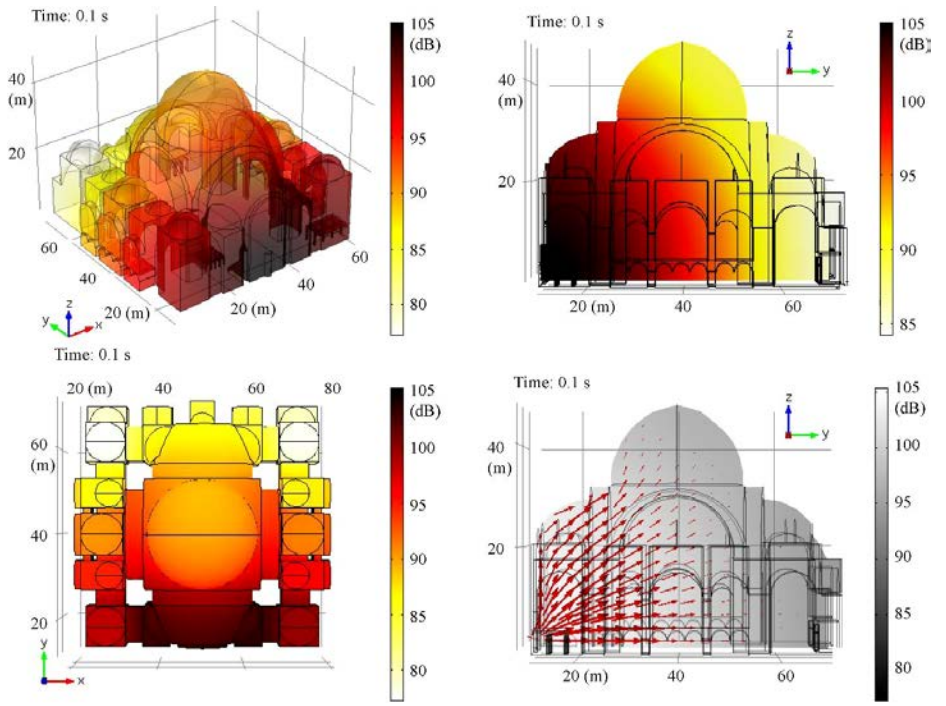

Fig. 3. Diffusion equation model results, spatial sound energy distributions and flow vectors for 250 Hz, time: 0.1 sec.

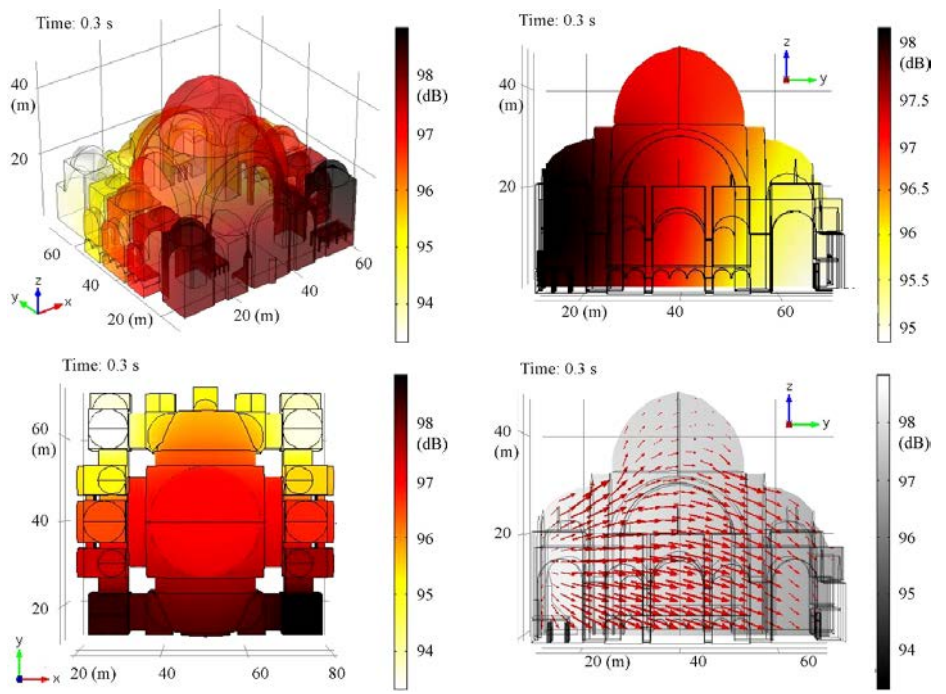

Fig. 4. Diffusion equation model results, spatial sound energy distributions and flow vectors for 250 Hz, at a time instance of 0.3 sec.

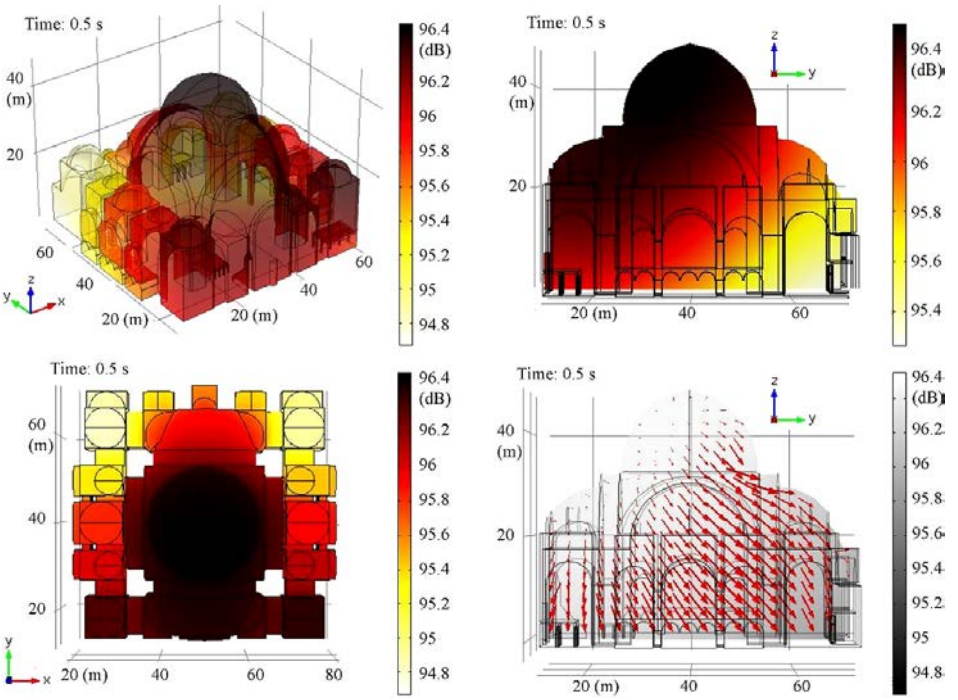

Fig. 5. Diffusion equation model results, spatial sound energy distributions and flow vectors for 250 Hz, at a time instance of 0.5 sec.

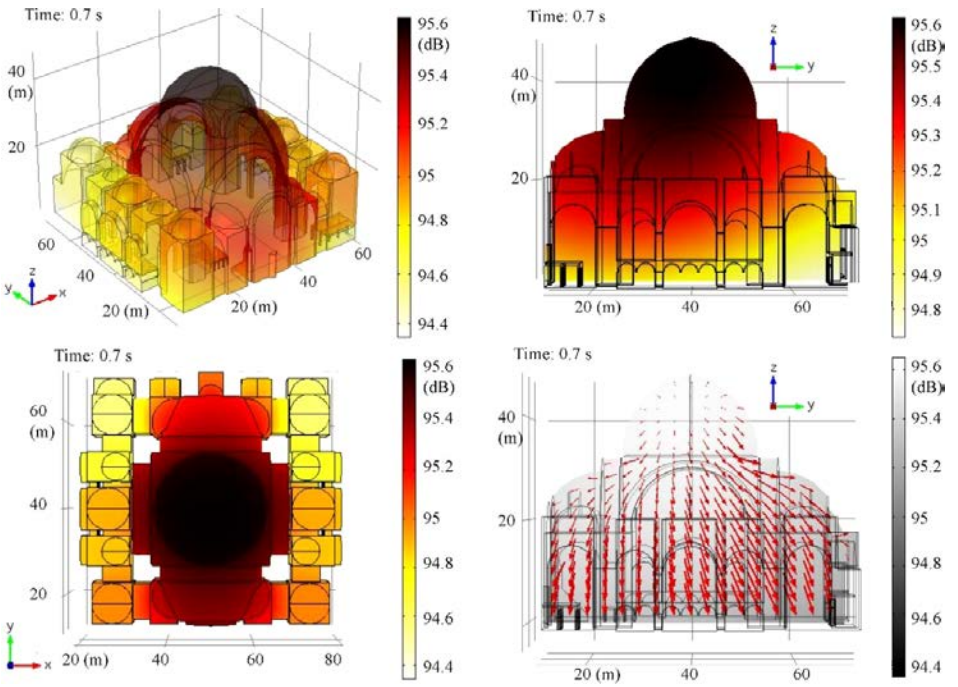

Fig. 6. Diffusion equation model results, spatial sound energy distributions and flow vectors for 250 Hz, at a time instance of 0.7 sec.

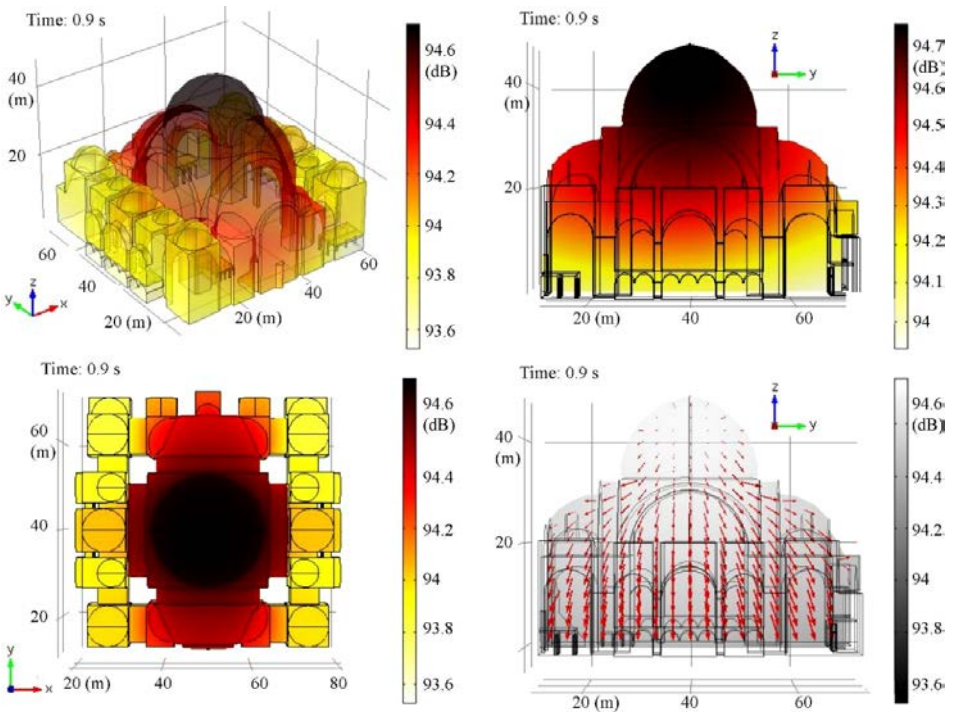

Fig. 7. Diffusion equation model results, spatial sound energy distributions and flow vectors for 250 Hz, at a time instance of 0.9 sec.

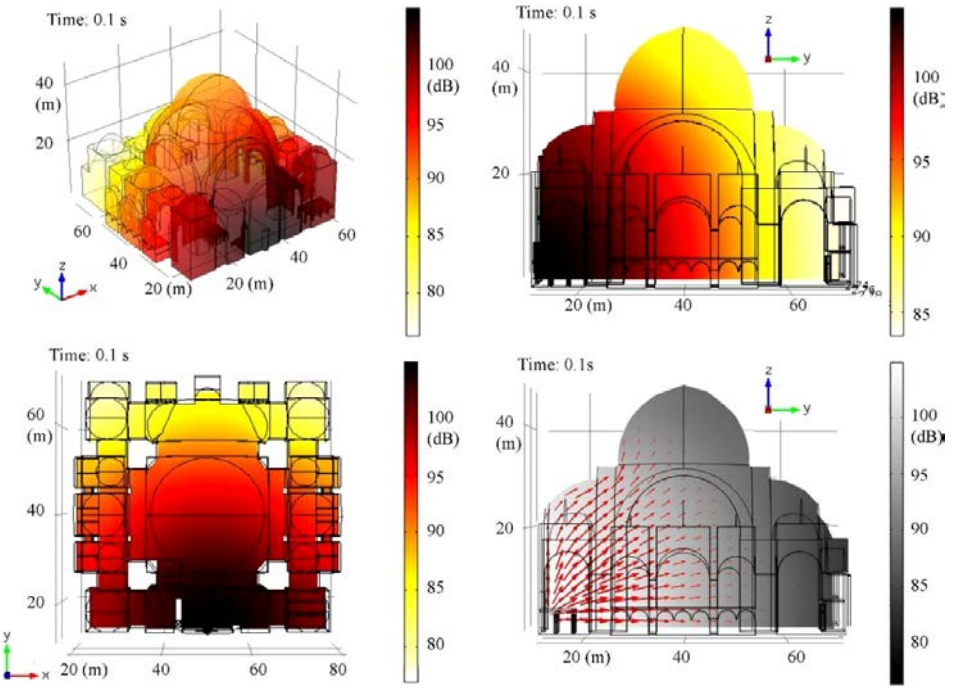

Fig. 8. Diffusion equation model results, spatial sound energy distributions and flow vectors for 1 kHz, time: 0.1 sec.

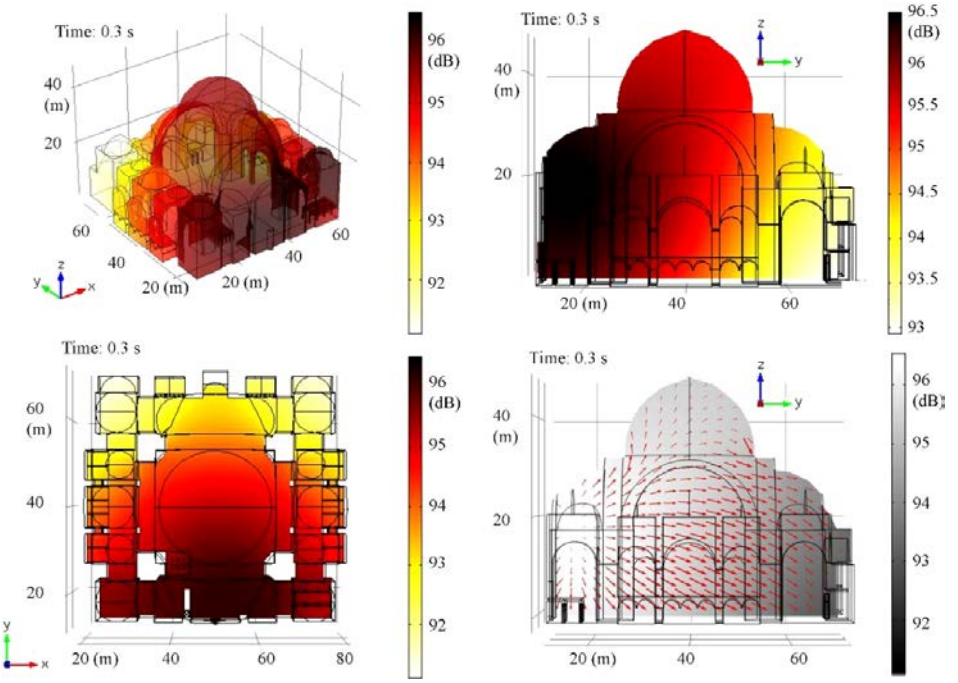

Fig. 9. Diffusion equation model results, spatial sound energy distributions and flow vectors for 1 kHz, time: 0.3 sec.

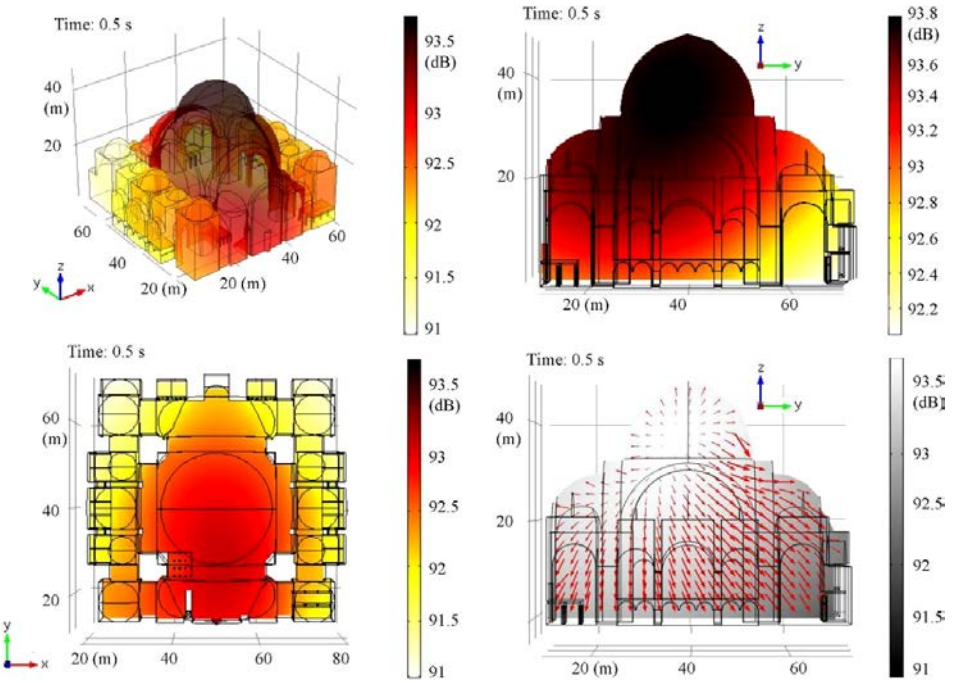

Fig. 10. Diffusion equation model results, spatial sound energy distributions and flow vectors for 1 kHz, time: 0.5 sec.

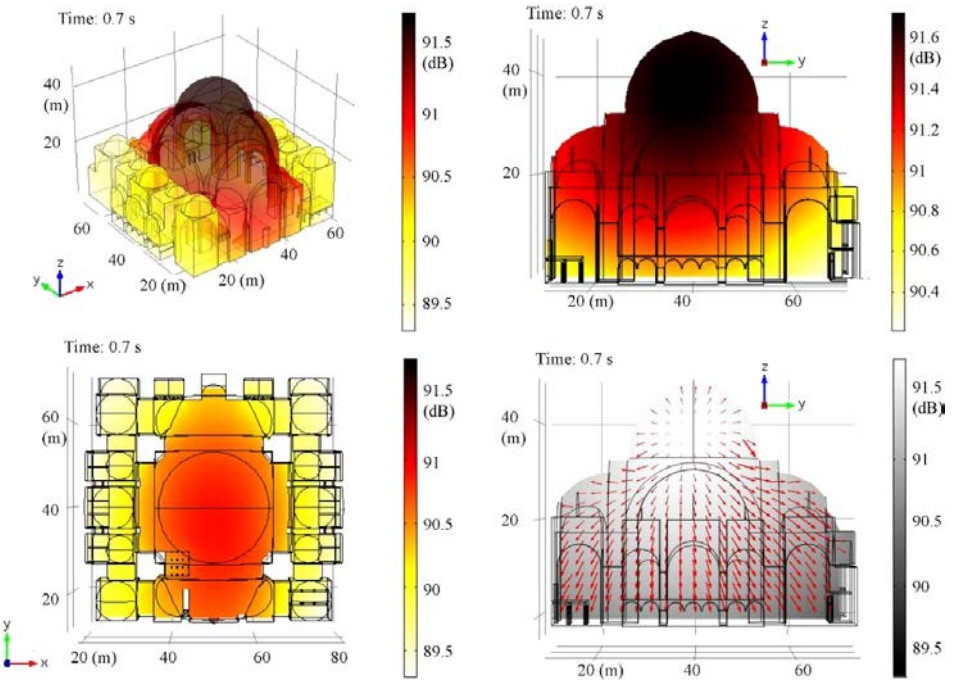

Fig. 11. Diffusion equation model results, spatial sound energy distributions and flow vectors for 1 kHz at a time instance of 0.7 sec.

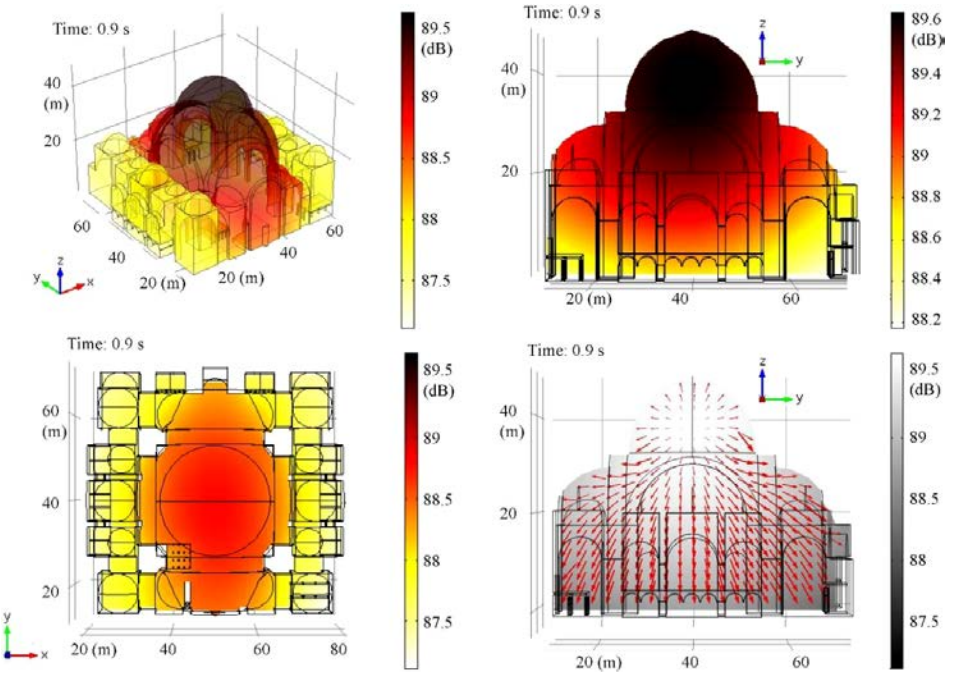

Fig. 12. Diffusion equation model results, spatial sound energy distributions and flow vectors for 1 kHz, at a time instance of 0.9 sec.

hall, while, at this point the central dome and back wall aisles have not been completely filled with sound energy. The zones closer to the floor (receiver/prayer heights) underneath the central dome in this period receive more energy compared to prayer locations in front of the back wall and other locations underneath the back wall corner domes and the upper back half of the central dome.

From Figs. 4–7, the initial time steps of the energy density distribution and energy flows are depicted after the source is terminated, with a time step of 0.2 sec including time instances of: 0.3 sec, 0.5 sec, 0.7 sec and 0.9 sec. In the first time steps, the flow vectors are directed towards the *mihrab* wall to the upper central dome and at the end all are pointed back towards the prayer floor, which is the energy scarce zone at that time period. From this point out, the energy center is the central dome, with its comparatively reflective surfaces and focusing geometry.

Figure 7 shows that the energy within that period is concentrated at the central axis underneath the main dome and semi-domes. It is beneficial that the dome focusing area is located well above the receiver height. On the other hand, this energy accumulation center keeps feeding energy back to the floor area, as can be observed from sound energy flow vectors. Furthermore, the side aisles underneath secondary domes get less energy compared to the *mihrab* wall section.

From Figs. 8–12, spatial sound energy level distributions from the DEM are illustrated by volume and slice plots as well as flow vectors/array plots for 1 kHz. Figure 8, illustrating the time step 0.1 sec, shows the ignition of the impulsive sound source. The initial time steps after termination of the source signal are provided from Figs. 9–11, including time steps 0.3 sec, 0.5 sec and 0.7 sec. In this time period, the energy flow vectors return from the dome towards the prayer floor. After the time instant 0.9 sec (Fig. 12), the flow vector patterns are similar, again indicating the central dome as an energy concentration zone.

For 1 kHz, the behavior of energy distribution densities and energy flow patterns is similar to the solution for 250 Hz. The major differences are the time of energy returns and the duration of the sound energy decay. As expected, the lower reverberation time at 1 kHz in comparison to 250 Hz, results in an earlier flow vector returns and a shorter duration of the whole decay process. This frequency dependence is due to the boundary absorption assignment. The absorptive carpet and reflective upper shell structure — including walls — together with the dominant geometrical features cause different energy flow characteristics for different frequency bands. The main advantage of providing spatial sound energy distribution plots is to better visualize the sound energy flows. Rather than the sound energy level differences (or absolute difference between the maximum and the minimum in dB), the pattern of energy flows within the volume is sought. Regardless of the magnitude of this absolute difference in sound energy levels, the energy would still drain from the energy dense volume/zone to the scarce zone. The asymmetric distribution of this energy zoning inside the structure contributes to the overlapping of early and late energy decays, particularly closer to the floor.

5. Conclusion

In this study, the diffusion equation model (DEM) is solved over a historically significant worship space. The simulation results are significant in examining the three-dimensional sound field of this existing monumental structure using spatial sound energy density distribution and flow vector analysis. It should be emphasized that the DEM, as applied by finite element modeling, is a practical and scientific method of room acoustic predictions, particularly for in-depth sound field analysis restricted to the reverberation process. As an outcome of this study, the unique application of the DEM over an existing structure, will motivate the use of this new tool for room acoustics estimations whether in design of virtual spaces (concept designs), or for renovation of existing spaces.

References

1. W. C. Sabine, *Collected Papers on Acoustics* (Harvard University Press, Cambridge, 1922).
2. C. F. Eyring, Reverberation time in dead rooms, *J. Acoust. Soc. Am.* **168** (1930) 217–241.
3. C. M. Harris, Application of wave theory of room acoustics to the design of auditoriums, *Ann. Phys.* **192**(1) (1989) 59–65.
4. D. Botteldooren, Finite-difference time-domain simulation of low-frequency room acoustic problems, *J. Acoust. Soc. Am.* **98** (1995) 3302–3308.
5. M. Aretz and M. Vorländer, Efficient modelling of absorbing boundaries in room acoustic FE simulations, *Acta Acust. United With Acust.* **96** (2010) 1042–1050.
6. L. Savioja and U. P. Svensson, Overview of geometrical room acoustics modeling techniques, *J. Acoust. Soc. Am.* **138** (2015) 708–730.
7. J. H. Rindel, The use of computer modeling in room acoustics, *J. Vibr. Eng.* **3**(4) (2000) 219–224. (Index 41–72 Paper of the International Conference BALTIC-ACOUSTIC 2000/ISSN 1392-8716).
8. E. N. Wester and B. R. Mace, A statistical analysis of acoustical energy flow in two coupled rectangular rooms, *Acta Acust.* **84** (1998) 114–121.
9. H. Kuttruff, *Room Acoustics*, 5th edn. (Spon Press, London, 2009).
10. J. Kang, Reverberation in rectangular long enclosures with diffusely reflecting boundaries, *Acta Acust. United With Acust.* **88** (2002) 77–87.
11. H. Zhang, Relaxation of sound fields in rooms of diffusely reflecting boundaries and its application in acoustical radiosity simulation, *J. Acoust. Soc. Am.* **119** (2006) 2189–2200.
12. F. Ollendorff, Statistical room-acoustics as a problem of diffusion: A proposal, *Acustica* **21** (1969) 236–245.
13. V. Valeau, J. Picaut and M. Hodgson, On the use of a diffusion equation for room-acoustic prediction, *J. Acoust. Soc. Am.* **119**(3) (2006) 1504–1513.
14. A. Billon, V. Valeau, A. Sakout and J. Picaut, On the use of a diffusion model for acoustically coupled rooms, *J. Acoust. Soc. Am.* **120**(4) (2006) 2043–2054.
15. Y. Jing and N. Xiang, On boundary conditions for the diffusion equation in room acoustic prediction: Theory, simulations, and experiments, *J. Acoust. Soc. Am.* **123**(1) (2008) 145–153.
16. P. Luizard, J.-D. Polack and B. F. G. Katz, Sound energy decay in coupled spaces using a parametric analytical solution of a diffusion equation, *J. Acoust. Soc. Am.* **135** (2014) 2765–2776.
17. Y. Jing, E. Larsen and N. Xiang, One-dimensional transport equation models for sound energy propagation in long spaces: Theory, *J. Acoust. Soc. Am.* **127** (2010) 2312–2322.

18. Y. Jing and N. Xiang, One-dimensional transport equation models for sound energy propagation in long spaces: Simulations and experimental results, *J. Acoust. Soc. Am.* **127** (2010) 2323–2331.
19. T. Polles, J. Picaut, M. Berengier and C. Bardos, Sound field modeling in a street canyon with partially diffusely reflecting boundaries by the transport theory, *J. Acoust. Soc. Am* **116** (2004) 2969–2983.
20. J. M. Navarro, F. Jacobsen, J. Escolano and J. J. López, A theoretical approach to room acoustic simulations based on a radiative transfer model, *Acta Acust. United With Acust.* **96** (2010) 1078–1089.
21. J. M. Navarro, J. Escolano and J. J. Lopez, Implementation and evaluation of a diffusion equation model based on finite difference schemes for sound field prediction in rooms, *Appl. Acoust.* **73** (2012) 659–665.
22. N. Xiang, J. Escolano, J. M. Navarro and Y. Jing, Investigation on the effect of aperture sizes and receiver positions in coupled rooms, *J. Acoust. Soc. Am.* **133**(6) (2013) 3975–3985.
23. T. N. Narasimhan, The dichotomous history of diffusion, *Phy. Today* **62**(7) (2009) 48–53. (2009 American Institute of Physics, S-0031-9228-0907-030-6/ISSN 0031-922).
24. R. Pierrat, J. J. Greffet and R. Carminati, Photon diffusion coefficient in scattering and absorbing media, *J. Opt. Soc. Am.* **23** (2006) 1106–1110.
25. J. Picaut, L. Simon and J. D. Polack, A mathematical model of diffuse sound field based on a diffusion equation, *Acta Acust.* **83** (1997) 614–621.
26. Y. Jing and N. Xiang, A modified diffusion equation for room-acoustic predication (L), *J. Acoust. Soc. Am.* **121**(6) (2007) 3284–3287.
27. A. Billon, J. Picaut and A. Sakout, Prediction of the reverberation time in high absorbent room using a modified-diffusion model, *Appl. Acoust.* **69** (2008) 68–74.
28. Y. Jing and N. Xiang, Visualizations of sound energy across coupled rooms using a diffusion equation model, Express Letter, *J. Acoust. Soc. Am.* **124**(6) (2008) 360–365.
29. N. Xiang, Y. Jing and A. C. Bockman, Investigation of acoustically coupled enclosures using a diffusion-equation model, *J. Acoust. Soc. Am.* **126**(3) (2009) 1189–1198.
30. J. Escolano, J. M. Navarro and J. J. López, On the limitation of a diffusion equation model for acoustic predictions of rooms with homogeneous dimensions, Letter to the Editor, *J. Acoust. Soc. Am.* **128**(4) (2010) 1586–1589.
31. C. Visentin, N. Prodi, V. Valeau and J. Picaut, A numerical investigation of the Fick's law of diffusion in room acoustics, *J. Acoust. Soc. Am.* **132** (2012) 3180–3189.
32. P. M. Morse and H. Feshbach, *Methods of Theoretical Physics* (McGraw-Hill, New York, 1953).
33. Z. Sü Gül, N. Xiang and M. Çalışkan, Investigations on sound energy decays and flows in a monumental mosque, *J. Acoust. Soc. Am.* **140**(1) (2016) 344–355.